Preprint Series

A Finite Element Plate Formulation for the Acoustical Investigation of Thin Air Layers

Ping Rong, Otto von Estorff

Institute of Modelling and Computation, Hamburg University of Technology

Loris Nagler, Martin Schanz

Institute of Applied Mechanics, Graz University of Technology

Abstract

Double wall systems consisting of thin plates separated by an air gap are common light-weighted wall structures with high transmission loss. Generally, these plate-like structures are modelled in a finite element analysis with shell elements and volume elements for the air (fluid) layer. An alternative approach is presented in this paper, using shell elements for the air layer as well. Firstly, the element stiffness matrix is obtained by removing the thickness dependence of the variational form of the Helmhotz equation by use of a power series. Secondly, the coupling between the acoustical shell element and the elastic structure is described. To verify the new shell element, a simple double wall system is considered. Comparing the predicted sound field with the results from a commerical FE software (with a single layer of volume elements) a very good agreement is observed. At the same time, employing the new elements with a 3rd order power series (4 DOFs per node), the calculation time is reduced.

1 Introduction

A double wall is a common structure in many industries, as it combines high stiffness with low specific weight. An example ist the fuselage of an aircraft with its outer aluminium and inner trim panels. From an acoustical point of view, such double partitions offer superior transmission loss compared to single partitions of comparable weight and stiffness [1]. In order to find an acoustically optimal wall design with predefined mechanical properties, experimental tests such as ISO 140 can be used. However, these can be both time consuming and expensive, depending on the efford needed to manufacture wall structures of varying parameters like the wall thicknesses, number and position of stiffeners, cavity depth, etc. Fortunately, a number of numerical techniques are available to predict the behavior of mechano-acoustical systems, the most popular one being the finite element method (FEM) [10].

Typical light-weighted double walls like the aforementioned aircraft fuselage have characteristic properties which can be exploited to simplify the respective FE models. Most importantly, they consist of structural subsystems, i.e., the walls, with thicknesses very small compared to the other dimensions. Consequently, if such a thin structure had to be discretized with volume (solid) elements, the dimensions of elements had to be kept in suitable proportion. This would lead to a large number of the degrees of freedom. Therefore, shell elements are used allowing for an accurate description of the mechanical behavior of the structure with significantly less elements (hence degrees of freedom) compared to volume elements. In practice, one is able to efficiently simulate plate-like structures with the given computational resources only by this means . There are a number of different types of shell elements used in FE simulations. For homogeneous elastic plates, the Love-Kirchhoff and Mindlin-Reissner plate theories[2]'[3] are used. Methods for describing sandwich plates by shell elements are under investigation[4]. Furthermore, shell elements can be used to model poroelastic plates[5] by applying the theory of elastic waves in porous solids[6, 7, 8]. In the study of vibro-acoustical properties of double wall systems with FEM these shell elements have been widely utilized. However, in most models the air layer or any other type of medium which can be modelled by an equivalent fluid, such as most flow resistivity type absorbers, is still modeled with volume elements. In order to reach a more unified description of double wall systems with a potential for a more efficient calculation, a 2D formulation of a thin layer of air will be developed in this work.

The outline of this paper is as follows: Firstly, an FE formulation of an acoustical shell element will be introduced, then the boundary conditions of this element will be discussed. Secondly, the coupling between the air layer and the structure will be investigated. Lastly, the acoustical shell element is used in a simple double wall system and the accuracy of the numerical results is verified by comparison with a "classical" 3-D model.

2 Formulation of an acoustical shell element

This section discusses the 2-D formulation of a thin layer of air in the frame of the finite element analysis.

2.1 2-D formulation of the air layer

The domain of the air (fluid) layer is considered to be plate-like, hence to have a relatively small extension in the thickness direction x_3 compared to its in-plane dimensions (x_1, x_2), i.e.,

$$\Omega = [(x_1, x_2, x_3) \in \mathbb{R}^3 \mid x_3 \in \left[-\frac{h}{2}, \frac{h}{2} \right], (x_1, x_2) \in A \subset \mathbb{R}^2], \tag{1}$$

with Ω being the domain of the air plate, x_i the coordinates in a Cartesian coordinate system, h the thickness, and A the midplane of the layer. In the following, the notation Γ will be used to indicate the boundary surface of the domain Ω. Furthermore, B denotes the lateral faces of Γ, and C the border line of A. The subscript $(\cdot)_i$ marks the vector component with respect to the direction x_i and $(\cdot)_{,i}$ and $(\cdot)_{,ii}$ denote the operators $\frac{\partial}{\partial x_i}$ and $\frac{\partial^2}{\partial x_i^2}$, respectively. Such a layer is depicted in fig. 1. If one assumes that the fluid medium is homogeneous and compressible, then
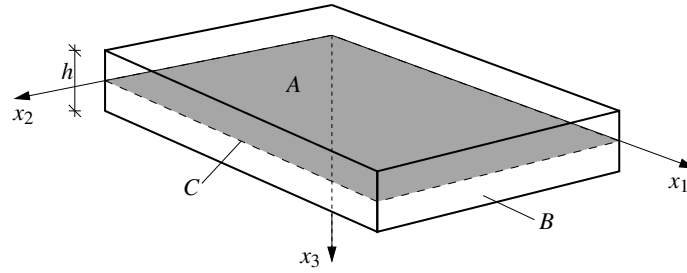
Figure 1: A plate-like layer of air or other acoustical fluid medium.

the governing equation (assuming harmonic exitation) for the wave propagation is the Helmholtz equation

$$\nabla^2 p + k^2 p = 0, \tag{2}$$

with p being the acoustic pressure, $k = \frac{\omega}{c}$ the wave number, ω the angular frequency, and c the speed of sound. Since the acoustical layer in a double wall system is generally enclosed by structures, it can be regarded as an interior problem. The respective variational formulation of the Helmholtz equation can be deduced by the standard method

$$\int_{\Omega} \left[\nabla p \cdot \nabla \bar{p} - k^2 p \bar{p} \right] dV + \int_{\Gamma_R} ik\beta p \bar{p} \, dS + \int_{\Gamma_N} (p_{,i} \cdot n_i) \bar{p} \, dS = 0, \tag{3}$$

where Γ_N are the boundary surfaces with Neumann boundary conditions and Γ_R those with Robin boundary condition. Furthermore, $\bar{p}$ indicates the test-function of the sound pressure, β the acoustical admittance, and the term $(p_{,i} \cdot n_i)$ represents the pressure gradient on Γ_N normal to the considered surface. Due to the plate-like geometry, the domain integral in (3) can be split into two parts, knowing that

$$\int_{\Omega} (\cdot) \, dV = \int_A \int_h (\cdot) \, dx_3 \, dA. \tag{4}$$

Similarly, the boundary integral can be split into an integral over the lateral faces and the upper and lower faces at $x_3 = \pm h/2$,

$$\int_{\Gamma_N} (\cdot)\, \mathrm{d}S = \int_{A^\pm} (\cdot)\, \mathrm{d}S + \int_C \int_h (\cdot)\, \mathrm{d}x_3\, \mathrm{d}C,\tag{5}$$

where the superscript $(\cdot)^\pm$ denotes the terms related to the upper and lower face of the plate, respectively. It is obvious that the integration with respect to x_3 is now separated from the integration in the x_1-x_2 plane. In order to eliminate the dependency on x_3, the thickness direction, the sound pressure p and its test function $\bar p$ are replaced by power series in x_3, such that

$$p(x_1,x_2,x_3) = \sum_{m=0}^{\infty} \overset{m}{p}(x_1,x_2)x_3^m\,,\tag{6a}$$

$$\bar p(x_1,x_2,x_3) = \sum_{\ell=0}^{\infty} \overset{\ell}{\bar p}(x_1,x_2)x_3^\ell\,.\tag{6b}$$

Then, by evaluating the integrations over h in equations (4) and (5), the dependency of the variational formulation on the x_3 coordinate is removed. However, new unknown quantities of the order ℓ and m, namely, $\overset{\ell}{\bar p}$ and $\overset{m}{p}$, are introduced, which only depend on the two in-plane coordinates x_1 and x_2. For the sake of easy reading, the subscript $(\cdot)_\alpha$ will be used in the following to denote functions that are only related to x_1 and x_2.

Since the assembly of the FE system matrix depends only on the domain integration, the plate-like formulation in the acoustical domain is derived first, whereas the boundary conditions will be considered in the section 2.2.

Substituting the test function $\bar p$ in the domain integration with the polynomial series (6b) yields

$$\int_\Omega \left[(\nabla p_\alpha \nabla \bar p_\alpha + p_{,3}\bar p_{,3}) - k^2 p\bar p \right] \mathrm{d}V =$$

$$\sum_{\ell=0}^{\infty} \int_A \left[\left(\overset{\ell}{G}_\alpha \nabla \overset{\ell}{\bar p}_\alpha + \ell \cdot \overset{\ell-1}{G}_3 \overset{\ell}{\bar p}_\alpha \right) - k^2 \overset{\ell}{H} \overset{\ell}{\bar p}(x_1,x_2) \right] \mathrm{d}S\,,\tag{7}$$

where

$$\overset{\ell}{G}_\alpha = \int_h \nabla p_\alpha x_3^\ell\, \mathrm{d}x_3\,, \qquad \overset{\ell}{G}_3 = \int_h p_{,3} x_3^\ell\, \mathrm{d}x_3\,, \qquad \overset{\ell}{H} = \int_h p x_3^\ell\, \mathrm{d}x_3\,.\tag{8}$$

It can be seen that the primary function p and the variable x_3 only appear in $\overset{\ell}{G}$ and $\overset{\ell}{H}$. Similarly, by substituting the power series (6a) into the equations (8), the integration from $-\frac{h}{2}$ to $\frac{h}{2}$ can be derived. As shown next, the resultants $\overset{\ell}{G}$ and $\overset{\ell}{H}$ can be represented in polynomial form as well,

one obtains

$$\overset{\ell}{G}_\alpha = \int\limits_h \nabla p_\alpha x_3^\ell \, dx_3 = \sum_{m=0}^\infty \nabla \overset{m}{p}_\alpha \cdot \frac{h}{m+\ell+1}\left(\frac{h}{2}\right)^{m+\ell} \frac{[1+(-1)^{m+\ell}]}{2} \tag{9a}$$

$$\overset{\ell}{G}_3 = \int\limits_h p_{,3} x_3^\ell \, dx_3 = \sum_{m=0}^\infty \overset{m}{p}_\alpha \cdot \frac{2m}{m+\ell}\left(\frac{h}{2}\right)^{m+\ell} \frac{[1-(-1)^{m+\ell}]}{2} \tag{9b}$$

$$\overset{\ell}{H} = \int\limits_h p x_3^\ell \, dx_3 = \sum_{m=0}^\infty \overset{m}{p}_\alpha \cdot \frac{h}{m+\ell+1}\left(\frac{h}{2}\right)^{m+\ell} \frac{[1+(-1)^{m+\ell}]}{2}. \tag{9c}$$

By substituting the equation (9) into the domain integration (7), the variational formulation of the "air-plate" is completed. However, before this can be used in the assembly of the system matrix, the power series needs to be truncated. In the literature[5],[9] it has been shown that only very few coefficients of (6) are required to adequately model even relatively thick layers. It is suggested that a third order polynomial ($\ell, m = 0, 1, 2, 3$) provides sufficient accuracy, in fact, such a trunction represents a cubic pressure distribution over the thickness. The respective integrands of (7) for this truncation are shown in equation (10), where the factor $\tilde{c}^2 = \frac{h^2}{12}$ is used.

$\ell = 0$:

$$\int\limits_A \left[h\left(\nabla \overset{0}{p}_\alpha + \tilde{c}^2 \nabla \overset{2}{p}_\alpha\right)\nabla \overset{0}{\bar{p}}_\alpha - hk^2\left(\overset{0}{p} + \tilde{c}^2 \overset{2}{p}\right)\overset{0}{\bar{p}} \right] dS \tag{10a}$$

$\ell = 1$:

$$\int\limits_A \left[h\left(\tilde{c}^2 \nabla \overset{1}{p}_\alpha + \frac{9}{5}\tilde{c}^4 \nabla \overset{3}{p}_\alpha\right)\nabla \overset{1}{\bar{p}}_\alpha + h\left(\overset{1}{p} + 3\tilde{c}^2 \overset{3}{p}\right)\overset{1}{\bar{p}} - hk^2\left(\tilde{c}^2 \overset{1}{p} + \frac{9}{5}\tilde{c}^4 \overset{3}{p}\right)\overset{1}{\bar{p}} \right] dS \tag{10b}$$

$\ell = 2$:

$$\int\limits_A \left[h\left(\tilde{c}^2 \nabla \overset{0}{p}_\alpha + \frac{9}{5}\tilde{c}^4 \nabla \overset{2}{p}_\alpha\right)\nabla \overset{2}{\bar{p}}_\alpha + 4h\tilde{c}^2 \overset{2}{p}\overset{2}{\bar{p}} - hk^2\left(\tilde{c}^2 \overset{0}{p} + \frac{9}{5}\tilde{c}^4 \overset{2}{p}\right)\overset{2}{\bar{p}} \right] dS \tag{10c}$$

$\ell = 3$:

$$\int\limits_A \left[h\left(\frac{9}{5}\tilde{c}^4 \nabla \overset{1}{p}_\alpha + \frac{27}{7}\tilde{c}^6 \nabla \overset{3}{p}_\alpha\right)\nabla \overset{3}{\bar{p}}_\alpha + h\left(\tilde{c}^2 \overset{1}{p} + \frac{27}{5}\tilde{c}^4 \overset{3}{p}\right)\overset{3}{\bar{p}} - hk^2\left(\frac{9}{5}\tilde{c}^4 \overset{1}{p} + \frac{27}{7}\tilde{c}^6 \overset{3}{p}\right)\overset{3}{\bar{p}} \right] dS. \tag{10d}$$

It should be noticed that due to the approximation using series expansion the original pressure variable p is not occurring any more, instead the system has to be solved for the coefficients $\overset{\ell}{p}$. In a third order approximation these coefficients are $\overset{0}{p}$, $\overset{1}{p}$, $\overset{2}{p}$ and $\overset{3}{p}$. According to the standard FEM procedure, both the primary and the test functions in an element are replaced by corresponding shape function φ. By use of equation (10) and the domain integral (7), the left hand side of the

FE system of third order can be rearranged, leading to

$$
\begin{bmatrix}
\mathbf{K}^{00} & 0 & \mathbf{K}^{02} & 0 \\
0 & \mathbf{K}^{11} & 0 & \mathbf{K}^{13} \\
\mathbf{K}^{20} & 0 & \mathbf{K}^{22} & 0 \\
0 & \mathbf{K}^{31} & 0 & \mathbf{K}^{33}
\end{bmatrix}
\begin{bmatrix}
\overset{0}{\mathsf{p}} \\
\overset{1}{\mathsf{p}} \\
\overset{2}{\mathsf{p}} \\
\overset{3}{\mathsf{p}}
\end{bmatrix}
=
\begin{bmatrix}
\mathsf{f}^0 \\
\mathsf{f}^1 \\
\mathsf{f}^2 \\
\mathsf{f}^3
\end{bmatrix},
\tag{11}
$$

where

$$
\mathbf{K}^{00}_{ij} = h \int_{A_e} \nabla\varphi_j \nabla\varphi_i \, \mathrm{d}S - k^2 h \int_{A_e} \varphi_j \varphi_i \, \mathrm{d}S,
\tag{12a}
$$

$$
\mathbf{K}^{11}_{ij} = h \int_{A_e} \left(\tilde{c}^2 \nabla\varphi_j \nabla\varphi_i + \varphi_j \varphi_i \right) \mathrm{d}S - k^2 h \int_{A_e} \tilde{c}^2 \varphi_j \varphi_i \, \mathrm{d}S,
\tag{12b}
$$

$$
\mathbf{K}^{22}_{ij} = h \int_{A_e} \left(\frac{9}{5} \tilde{c}^4 \nabla\varphi_j \nabla\varphi_i + 4\tilde{c}^2 \varphi_j \varphi_i \right) \mathrm{d}S - k^2 h \int_{A_e} \frac{9}{5} \tilde{c}^4 \varphi_j \varphi_i \, \mathrm{d}S,
\tag{12c}
$$

$$
\mathbf{K}^{33}_{ij} = h \int_{A_e} \left(\frac{27}{7} \tilde{c}^6 \nabla\varphi_j \nabla\varphi_i + \frac{81}{5} \tilde{c}^4 \varphi_j \varphi_i \right) \mathrm{d}S - k^2 h \int_{A_e} \frac{27}{7} \tilde{c}^6 \varphi_j \varphi_i \, \mathrm{d}S,
\tag{12d}
$$

$$
\mathbf{K}^{02}_{ij} = \mathbf{K}^{20}_{ji} = h \int_{A_e} \tilde{c}^2 \nabla\varphi_j \nabla\varphi_i \, \mathrm{d}S - k^2 h \int_{A_e} \tilde{c}^2 \varphi_j \varphi_i \, \mathrm{d}S,
\tag{12e}
$$

$$
\mathbf{K}^{13}_{ij} = \mathbf{K}^{31}_{ji} = h \int_{A_e} \left(\frac{9}{5} \tilde{c}^4 \nabla\varphi_j \nabla\varphi_i + 3\tilde{c}^2 \varphi_j \varphi_i \right) \mathrm{d}S - k^2 h \int_{A_e} \frac{9}{5} \tilde{c}^4 \varphi_j \varphi_i \, \mathrm{d}S,
\tag{12f}
$$

and A_e being the area of an element.

2.2 Acoustical boundary conditions

The integration over the boundary surfaces of an acoustical layer is separated according to equation (5). The boundary condition can be either of Neumann or Robin type. The variational forms of both types of boundary conditions are demonstrated in equation (3). In general, the Neumann condition defines the particle velocity or pressure gradient on a certain area of the surface, which can induce an excitation of the system. The Robin boundary condition depends on the ratio of sound pressure to particle velocity, which defines the acoustical impedance. Both types of conditions can be evaluated through the integral over the surface of the air layer. Due to the geometry of the layer, the whole surface can be divided into two parts, as shown in equation (5). The first part includes the top and bottom face $A^{\pm}$, which are located at some constant distance from the middle surface. Hence, no integration over the thickness is involved in their evaluation. The second part, however, includes the lateral faces of the layer. In this case a procedure similar to the one used in 2.1 has to be applied to eliminate the variable x_3.

Firstly, the Neumann boundary condition is considered. The polynomial series (6) are again used to approximate the primary and test functions. On the surfaces $A^{\pm}$, x_3 has the constant

values $\pm\frac{h}{2}$. Therefore, the evaluation of the integral is straightforward, one obtains

$$\int\limits_{A^{\pm}} (p_{,i} \cdot n_i)\bar{p}\,\mathrm{d}S = \sum_{\ell=0}^{\infty} \left(\frac{h}{2}\right)^{\ell} \int\limits_{A} \left[(-1)^{\ell}(p_{,i} \cdot n_i)^{-} + (p_{,i} \cdot n_i)^{+}\right] \overset{\ell}{\bar{p}}_{\alpha}\,\mathrm{d}S. \tag{13}$$

The pressure gradients $(p_{,i} \cdot n_i)^{\pm}$ are mostly prescribed by the excitation on the surfaces $A^{\pm}$, which can be directly inserted. However, the boundary surface integral over the region B has to be reduced to a curve integral. By using the same method of separating the variable x_3 and integrating over the thickness, the boundary curve integral can be obtained as

$$\int\limits_{B} (p_{,i} \cdot n_i)^{b}\bar{p}\,\mathrm{d}S = \sum_{\ell=0}^{\infty} \int\limits_{C} \overset{\ell}{G}_b \overset{\ell}{\bar{p}}_{\alpha}\,\mathrm{d}C, \tag{14}$$

where

$$\overset{\ell}{G}_b = \int\limits_{h} (p_{,i} \cdot n_i)^{b} x_3^{\ell}\,\mathrm{d}x_3. \tag{15}$$

Although the boundary curve C is now given as a 1-D line, the Neumann data, $(p_{,i} \cdot n_i)^{b}$, has to be provided on the lateral faces B. In practice this can cause some inconveniences, since the purpose of the plate-like formulation is to exclude the dimension of the thickness. However, if it can be assumed that, due to thin thickness of the plate-like structure, the given pressure gradient on B is independent of x_3 it can be represented by its subset on the boundary curve C, $(p_{,i} \cdot n_i)^{c}$. Based on this assumption, equation (15) can be easily simplified to

$$\overset{\ell}{G}_b = (p_{,i} \cdot n_i)^{c}\frac{h}{\ell+1}\left(\frac{h}{2}\right)^{\ell}\frac{[1+(-1)^{\ell}]}{2}. \tag{16}$$

Furthermore, a truncation has to be carried out here as well. According to equations (13), (14), and (16) the terms of the third order truncation are presented by.

$$\ell = 0 : \quad \int\limits_{A} \left[\left(g^{+}+g^{-}\right)\overset{0}{\bar{p}}_{\alpha}\right]\mathrm{d}S + h\int\limits_{C} g^{c}\overset{0}{\bar{p}}_{\alpha}\,\mathrm{d}C, \tag{17a}$$

$$\ell = 1 : \quad \frac{h}{2}\int\limits_{A} \left[\left(g^{+}-g^{-}\right)\overset{1}{\bar{p}}_{\alpha}\right]\mathrm{d}S, \tag{17b}$$

$$\ell = 2 : \quad \frac{h^2}{4}\int\limits_{A} \left[\left(g^{+}+g^{-}\right)\overset{2}{\bar{p}}_{\alpha}\right]\mathrm{d}S + \frac{h^3}{12}\int\limits_{C} g^{c}\overset{2}{\bar{p}}_{\alpha}\,\mathrm{d}C, \tag{17c}$$

$$\ell = 3 : \quad \frac{h^3}{8}\int\limits_{A} \left[\left(g^{+}-g^{-}\right)\overset{3}{\bar{p}}_{\alpha}\right]\mathrm{d}S, \tag{17d}$$

where $g^{\pm} = (p_{,i} \cdot n_i)^{\pm}$ and $g^{c} = (p_{,i} \cdot n_i)^{c}$. As mentioned above, the prescribed pressure gradient can be regarded as excitation on the system. With equation (17) the right hand side entries of the

FE system (11) can be assembled, such that

$$f_i^0 = -\int_{A_e} (g^+ + g^-)\varphi_i \, dS - \int_{C_e} hg^c \varphi_i^c \, dC, \tag{18a}$$

$$f_i^1 = -\int_{A_e} \frac{h}{2}(g^+ - g^-)\varphi_i \, dS, \tag{18b}$$

$$f_i^2 = -\int_{A_e} \frac{h^2}{4}(g^+ + g^-)\varphi_i \, dS - \int_{C_e} \frac{h^3}{12} g^c \varphi_i^c \, dC, \tag{18c}$$

$$f_i^3 = -\int_{A_e} \frac{h^3}{8}(g^+ - g^-)\varphi_i \, dS, \tag{18d}$$

where φ^c is the shape function of the edge elements on the boundary curve C.

The impedance boundary condition can be deduced in the same manner. Firstly, the power series (6) are substituted into the integral over the boundary surfaces and curves, which yields

$$\int_{\Gamma_R} ik\beta p\bar{p} \, dS = \sum_{m=0}^{\infty} \sum_{\ell=0}^{\infty} ik\beta \left[\int_{A^{\pm}} \overset{m}{p}_\alpha \cdot \overset{\ell}{\bar{p}}_\alpha \left(\frac{h}{2}\right)^{m+\ell} \left[1 + (-1)^{m+\ell}\right] dS \right.$$
$$\left. + \int_{C} \overset{m}{p}_\alpha \cdot \overset{\ell}{\bar{p}}_\alpha \frac{h}{m+\ell+1} \left(\frac{h}{2}\right)^{m+\ell} \frac{[1 + (-1)^{m+\ell}]}{2} \, dC \right]. \tag{19}$$

By truncating equation (19), an additional system matrix can be created with respect to the Robin boundary condition. For the third order truncation this matrix is given by

$$\tilde{\mathbf{K}} = ik\beta \begin{bmatrix} \tilde{K}^{00} & 0 & \tilde{K}^{02} & 0 \\ 0 & \tilde{K}^{11} & 0 & \tilde{K}^{13} \\ \tilde{K}^{20} & 0 & \tilde{K}^{22} & 0 \\ 0 & \tilde{K}^{31} & 0 & \tilde{K}^{33} \end{bmatrix}, \tag{20}$$

where

$$\tilde{K}_{i,j}^{00} = \int_{A_e} 2 \cdot \varphi_j \varphi_i \, dS + \int_{C_e} h \cdot \varphi_j^c \varphi_i^c \, dC, \tag{21a}$$

$$\tilde{K}_{i,j}^{11} = \tilde{K}_{i,j}^{02} = \tilde{K}_{ji}^{20} = \int_{A_e} 6\tilde{c}^2 \cdot \varphi_j \varphi_i \, dS + \int_{C_e} h\tilde{c}^2 \cdot \varphi_j^c \varphi_i^c \, dC, \tag{21b}$$

$$\tilde{K}_{i,j}^{22} = \tilde{K}_{i,j}^{13} = \tilde{K}_{ji}^{31} = \int_{A_e} 18\tilde{c}^4 \cdot \varphi_j \varphi_i \, dS + \int_{C_e} \frac{9}{5} h\tilde{c}^4 \cdot \varphi_j^c \varphi_i^c \, dC, \tag{21c}$$

$$\tilde{K}_{i,j}^{33} = \int_{A_e} 54\tilde{c}^4 \varphi_j \varphi_i \, dS + \int_{C_e} \frac{27}{7} h\tilde{c}^6 \varphi_j^c \varphi_i^c \, dC. \tag{21d}$$

2.3 Air-structure coupling

In order to couple the air layer with the surrounding structure at its surfaces, suitable coupling conditions have to be formulated to guarantee equilibrium of stresses, continuity of displacements, and equilibrium of pressure at the interfaces. The coupling between three-dimensional elastic and acoustic continua has been presented in many publications[10]. Hereby the coupling conditions on the acoustic-elastic interface are

$$
\begin{aligned}
u_i^a n_i^a &= -u_i^e n_i^e \\
p^a n_i^a &= \sigma_{ij}^e n_j^e,
\end{aligned}
\tag{22}
$$

where u_i is the displacement and $\sigma_{ij}^e n_j^e$ the traction on the interface, the superscripts $(\cdot)^a$ and $(\cdot)^e$ denote the acoustical and elastic domain, respectively. For the structural part, the coupling term is derived from the traction (the pressure load). The same is applied to the acoustical part as a Neumann condition, which can be written as

$$
\begin{aligned}
p_{,i}^a n_i^a &= -\rho \dot{v}_i^a n_i^a \\
&= -\rho \ddot{u}_i^a n_i^a.
\end{aligned}
\tag{23}
$$

In the frequency domain the second order time-derivative becomes $\ddot{u}_i^a = -\omega^2 u_i^a$. Therefore, equation (23) can be rewritten as $p_{,i}^a n_i^a = \rho \omega^2 u_i^a n_i^a$. The governing relation of the coupling can be obtained by integrating equation (22) over the acoustic-elastic interface, such that

$$
I^{ae} = -\int_{\Gamma^{ae}} p^a \bar{u}_i^e n_i^a \, \mathrm{d}S^e - \omega^2 \rho \int_{\Gamma^{ae}} u_i^e n_i^e \bar{p}^a \, \mathrm{d}S^a.
\tag{24}
$$

The conditions for coupling the two-dimensional air plate with structures are obviously the same as for a three-dimensional coupling. In the former case, however, it must be accounted for the fact that the interfaces are located at a certain distance from the middle surfaces while the pressures incorporated into the formulation are solely defined on the middle surface itself. This requires to replace the pressure by the corresponding power series evaluated at the appropriate location.

It is assumed that the coupling interface is perpendicular to the x_3 axis and the structure is coupled on the surfaces, A^+ and A^-, of the acoustic layer. The distances of these surfaces to the middle surface are $\frac{h}{2}$ and $-\frac{h}{2}$, respectively. Therefore, the coupling integral in equation (24) becomes

$$
I^{ae} = -\sum_{\ell=0}^{\infty} \left[\int_{A^\pm} \left(\pm \frac{h}{2} \right)^\ell \overset{\ell}{p}{}^a \bar{u}_3^e \, \mathrm{d}S^e + \omega^2 \rho \int_{A^\pm} \left(\pm \frac{h}{2} \right)^\ell u_3^e \overset{\ell}{\bar{p}}{}^a \, \mathrm{d}S^a \right].
\tag{25}
$$

In view of a finite element discretization, the term of the ℓth order represents coupling matrices between the variables u^e and $\overset{\ell}{p}{}^a$ located at specific off-diagonal positions in the overall system matrix. Finally, the coupling formulation (25) has to be truncated according to the chosen order of approximation and the appropriate FE shape function for the acoustical and structural quantities have to be introduced.

3 Numerical example

In this section, a simple FE model of a double wall is used to verify the acoustical shell formulation of a thin air layer.

3.1 Model description
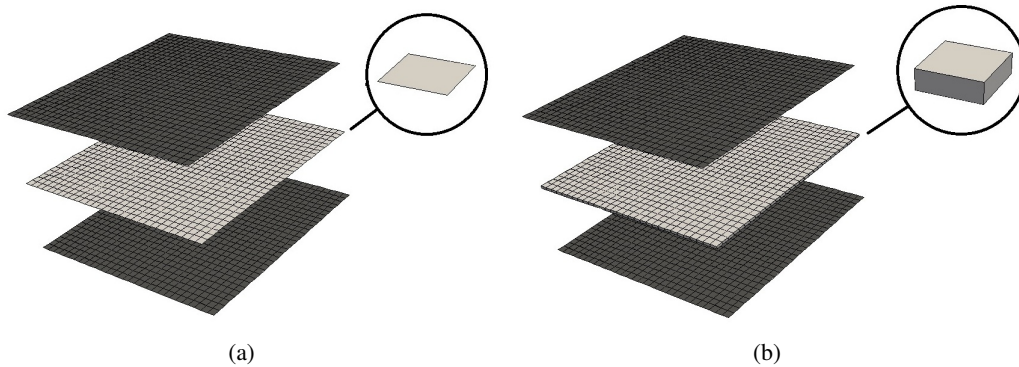
Figure 2: A simple double wall system consisting of two alumnium plates of 2 mm thickness (blue) and an 1 cm air gap (red). Modelled with three shell layers (a) or shells and volume elements for the air (b).

The modelled system consists of an air layer with thickness of 1 cm, which is placed between two aluminum plates of 2 mm thickness . These two elastic plates are modeled by the Mindlin formulation, and the air layer by the shell formulation described in section 2.1. Both elastic plates are coupled to the air-plate at the surfaces of $A^{\pm}$ by the method presented in section 2.3. A simply supported boundary condition is assumed on the edges of the elastic plates, which means the displacements are constrained while the rotations are free. As for the air-plate the impedance boundary condition is applied on its boundary, i.e., its edge and an acoustical admittance of $\beta = 1$ is selected implying a non-reflecting boundary. All three plates have the dimension 90 cm $\times$ 90 cm and are discretized with 30×30 bilinear Quad4 elements, as shown in fig. 2(a). The material properties Young's modulus of $7.24E10 \, \text{N/m}^2$ and density of $2770 \, \text{kg/m}^3$ have been used for the aluminum plates. The density of air is set to $1.209 \, \text{kg/m}^3$ and the speed of sound to $343.3 \, \text{m/s}$.

For comparison, a similar FE model is built with the commercial software Nastran[14]. Using the same material properties and boundary conditions, the plates are discretized with 30×30 elements as well. In order to avoid an overmuch distortion of volume elements, the air layer is modeled with one layer of 3-D elements only, $30 \times 30 \times 1$ Hex8 elements corresponding to the Quad4 shell elements. Based on the discretization, the ratio between the thickness of these 3-D elements and their edge length is $1 : 3$. In fig. 2(b) the mesh of the Nastran model is shown.

For the sake of consistency, the third order truncation is applied to the acoustical shell elements. Each node of the air-plate has 4 degrees of freedom (DOFs). The Nastran model has only one layer of acoustical elements with one DOF at each node. Thus, the total number of the
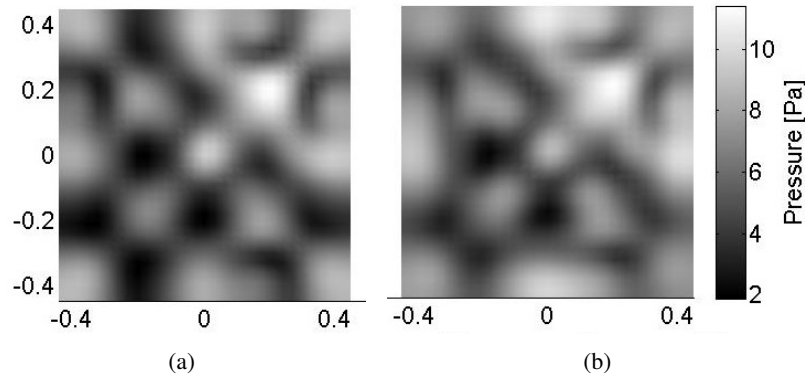
Figure 3: Sound pressure distribution at the interface between an 1cm air layer and two alu-
minium plates, at 300 Hz. (a): The result of the Nastran model on the surface of plate
#1 (excited plate). (b): The result of the air-plate model on the surface of plate #1.

DOFs is 9610 for the air-plate model and 7688 for the Nastran model. A vertical nodal force at
the position $(x_1, x_2) = (0.15\,\text{cm}, 0.15\,\text{cm})$ from the corner is set as the excitation on one of the
plates. In the following, this plate is hereafter referred as plate #1 while the other one is plate
#2.

3.2 Numerical results

The simulations are carried out with the harmonic excitations in the frequency range from 20 Hz
to 1 kHz with 5 Hz steps. In fig. 3, the predicted sound pressure distributions at 300 Hz are
illustrated. Fig. 3(a) shows the result of the Nastran model on the interface between the air
layer and the excited plate, while fig. 3(b) shows the respective result of the air-plate model.
Although the sound pressure in some areas appears to be slightly different, the patterns basically
agree fairly well with each other. It is noteworthy in the air-plate model that the sound pressure
on the interfaces is not directly obtained, but it is calculated during the post processing by re-
substituting the calculated sound pressure on the midplane back into the power series (6).

Since the air layer is coupled with the two plates, it is also of interest to examine the behavior
of both plates. The predicted displacements normal to the surface at 300 Hz are shown in fig. 4.
The high similarity between the predictions of both models is again observed. Small differences
can be found in the same regions where the sound fields differed, for example the upper right
section of plate #1. The difference between the results from both models can be caused not only
by the formulation of the 3-D air layer, but also by the formulation of the plate elements. In
fact, the exact implementation of the shell elements used in Nastran is unknown, although the
same parameters as for Mindlin plates are used in the calculation. Nevertheless, as being a wide-
spreaded commercial software the results of Nastran can still be regarded as a good reference.

In order to provide an overview of the results within the frequency range of the simulation, the
predicted sound pressure in the center point of the air layer is shown in fig. 5. In the frequency
range below 200 Hz, the results are almost identical. Only in the frequency region from 200 to

11
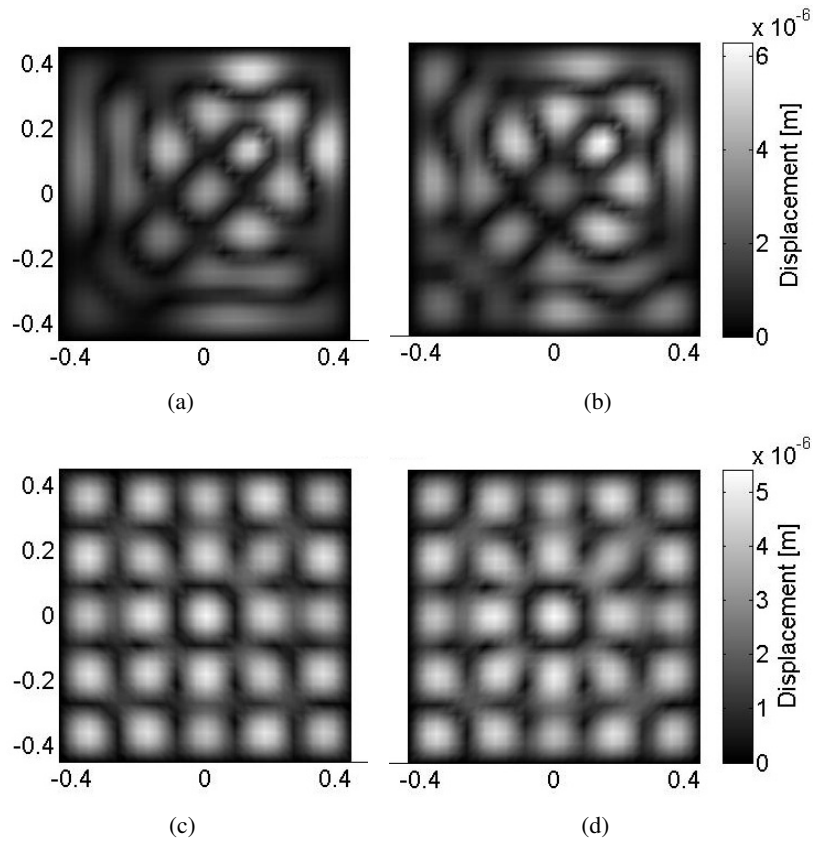
Figure 4: The predicted surface normal displacements of two aluminium plates separated by an air layer, at 300 Hz. (a): the result of the Nastran model of the plate #1. (b): the result of the air-plate model of the plate #1. (c): the result of the Nastran model of the plate #2. (d): the result of the air-plate model of the plate #2.
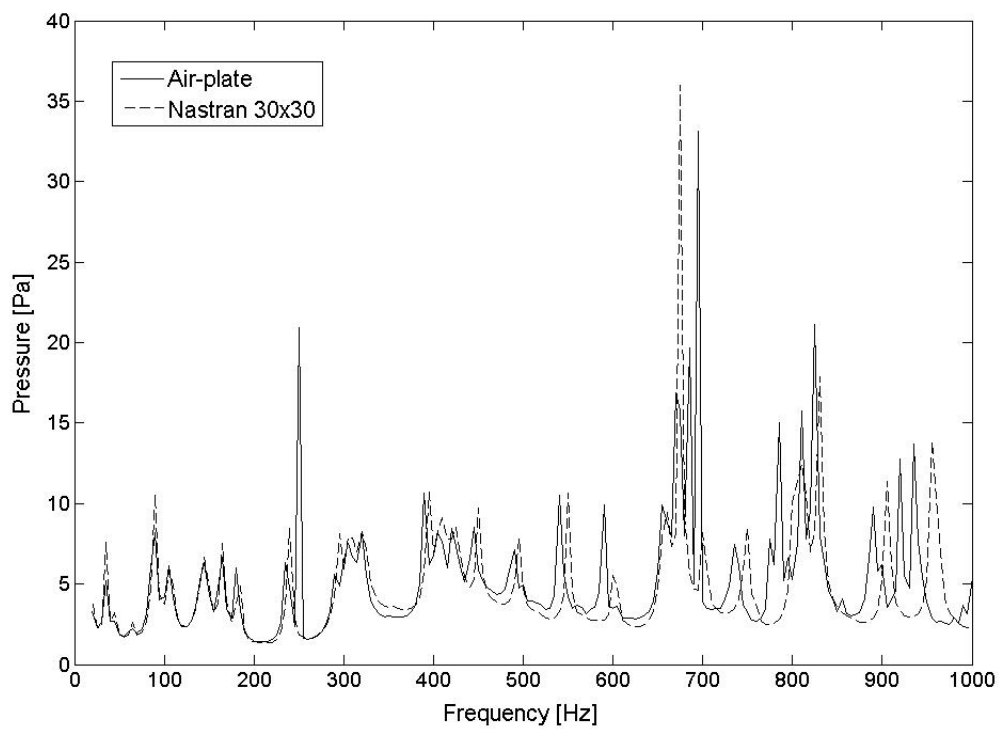
Figure 5: Predicted sound pressure in the middle of the air layer in the frequency range from 20 Hz to 1 kHz with 5 Hz step.

800 Hz the eigenfrequencies of the system are shifted by a small amount. It must be mentioned that the air-plate model using a cubic approximation is more than necessary because a linear approximation yields the same results. Hence, it can be concluded that the air-plate results are more reliable than those of the Nastran solution. The latter uses only one volume element over the thickness to keep the amount of DOFs in the same order as in the plate model. Usually, three layers of volume elements are recommended but this would result in a finer discretisation in plate direction to avoid distorted meshes. Certainly, both FE solutions decrease in accuracy for increasing frequency if the mesh size is kept constant.

The air-plate model is implemented with the open source FEM library libMesh[11] and the solver libraries PETSc[12] and SuperLU_DIST[13]. The average computation time for solving the Nastran model was 7.5 seconds per frequency and 7 seconds for the air-plate model. As mentioned above, the size and, consequently, the numerical effort of the air-plate system can be reduced by choosing a lower order approximation, e.g., a linear one, without changing the results. In this case, the computation time of the air-plate is reduced and out-performs the Nastran solution.

4 Conclusion

The finite element formulation of an acoustical shell element has been developed. Such a formulation can be useful for simulating the acoustical behavior of air layers. The discretization of structures with shell elements is usually much easier than with 3-D elements. In general, a 3-D simulation requires a relatively fine mesh to avoid excessive distortion of the elements. Also, the 2-D mesh can be reused easily when only the thickness of the layer is changed.

To derive the FE respresentation of the air layer, the variational form of the Helmholtz equation has been approximated by a power series leading to a 2-D form. The setup of the boundary conditions and the coupling between structural elements and acoustical shell elements were also introduced. For these couplings, the available formulations for 3-D elements could be adapted to the shell formulation.

In a numerical example, a simple double wall system has been used to compare the standard 3-D and the shell formulation. The model includes a thin layer of air that is coupled with two elastic plates, and non-reflecting impedance boundary conditions are imposed for the air layer. The results have shown very good agreement with even reduced computational costs.

A third order truncation has been used throughout this work. According to the thickness of the fluid layer and the required precision, different approximation orders of the power series can be used to suite the requirements. The truncation in a lower order can reduce the size of the system, while higher orders can provide more accuracy. Theoretically, the accuracy of the linear or the first order approximation suffice for the thin layer, while the high-order approximation is only required for relatively thick layer. The formulations with different approximation orders can be easily modified on the same frame. Further investigations are recommended in order to investigate the optimal approximation order of the air shell elements for different thickness where they might offer an even higher reduction in computational cost. Finally, using these elements for absorbing layers (sound absorption materials) would improve their usefulness in simulating realistic double wall set-ups.

References

[1] F. Fahy *Foundations of engineering acoustics,* (Academic Press, 2001).

[2] E. Reissner, Finite Deflections of Sandwich Plates, *J. Aero. Sci.* **15**(7), 435-440 (1948).

[3] R.D. Mindlin, Influence of Rotary Inertia and Shear on Flexural Motions of Isotropic, Elastic Plates, *Computers & Structures,* **18**, 31-38 (1951).

[4] K.H. Ha, Finite element analysis of sandwich plates: An overview, *J. App. Mech., Transactions of the ASME* **37**(4), 397-403 (1990).

[5] L. Nagler and M. Schanz, An extendable poroelastic plate formulation in dynamics, *Arch. App. Mech.* **80**, 1177-1195 (2010).

[6] M.A. Biot, General Theory of Three-Dimensional Consolidation, *J. of App. Phys.* **12**, 155-164 (1941).

[7] M.A. Biot, Theory of Propagation of Elastic Waves in a Fluid-Saturated Porous Solid.I. Low Frequency Range, *J. Acoust. Soc. Amer.* **28**(2), 168-178 (1956).

[8] M.A. Biot, Theory of Propagation of Elastic Waves in a Fluid-Saturated Porous Solid.II. Higher Frequency Range, *J. Acoust. Soc. Amer.* **28**(2), 179-191 (1956).

[9] L. Nagler, Simulation of Sound Transmission through Poroelastic Plate-like Structures, *Computation in Engineering and Science* **10**, (Verlag der Technischen Universität Graz, 2011).

[10] O.C. Zienkiewicz and R.L. Taylor, *The finite element Method (5th Edition), Vol.1: The basis* (Butterworth-Heinemann, 2000).

[11] B. S. Kirk, J. W. Peterson, R. H. Stogner, and G. F. Carey, libMesh: A C++ Library for Parallel Adaptive Mesh Refinement/Coarsening Simulations. *Engineering with Computers* **22**(3-4), 237-254 (2006).

[12] Mathematics and Computer Science Division, Argonne National Laboratory. *The portable, extensible, toolkit for scientific computation (PETSc). http://www.mcs.anl.gov/petsc.*

[13] X. Li and J. Demmel, *ACM Trans. Mathematical Software* **29**, 110-140 (2003).

[14] MSC Software, *MSC Nastran. http://www.mscsoftware.com* (2008).